Accepted Manuscript

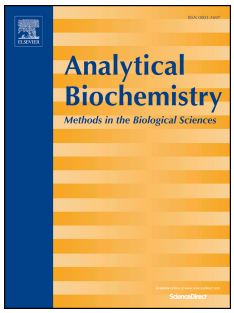

Single-wall carbon nanotube based electrochemical immunoassay for leukemia detection

Payal Gulati, Prabhjot Kaur, M.V. Rajam, Tapasya Srivastava, Prabhash Mishra, S.S. Islam

PII: S0003-2697(18)30442-1

DOI: 10.1016/j.ab.2018.07.020

Reference: YABIO 13088

To appear in: *Analytical Biochemistry*

Received Date: 26 December 2017

Revised Date: 2 July 2018

Accepted Date: 22 July 2018

Please cite this article as: P. Gulati, P. Kaur, M.V. Rajam, T. Srivastava, P. Mishra, S.S. Islam, Single-wall carbon nanotube based electrochemical immunoassay for leukemia detection, *Analytical Biochemistry* (2018), doi: 10.1016/j.ab.2018.07.020.

Single-wall carbon nanotube based electrochemical immunoassay for leukemia detection

Payal Gulati[a], Prabhjot Kaur[b], M.V. Rajam[b], Tapasya Srivastava[b], Prabhash Mishra[a], S.S. Islam[a*]

[a]Centre for Nanoscience and Nanotechnology, Jamia Millia Islamia (A Central University), New Delhi, India

[b]Department of Genetics, Delhi University, New Delhi, India

*Corresponding Author E-mail: sislam@jmi.ac.in (S.S. Islam).

Tel.: +91 11 26987153

Abstract

A label- free electrochemical immunosensor is fabricated using high quality single-walled carbon nanotube for early detection of leukemia cells. It is based on P-glycoprotein (P-gp) expression level detection; by effective surface immune-complex formation with the monoclonal anti-P-glycoprotein antibodies bound to an epoxy modified nanotube surface. The expression level of P-gp on the leukemia cell surface detected by cyclic voltammetry is in good agreement with immunofluorescence microscopy studies. The proposed biosensor could be used for the detection of P-gp expressing cells within a linear range of $1.5x10^3$ cells/ mL – $1.5x10^7$ cells/mL where lowest detection limit is found to be 19 cells/mL. A calibration plot of peak current v/s the logarithm of concentration of leukemia K562 cells is found linear with a regression coefficient of 0.935. This strategy promises high sensitivity, low- cost, fast, and repeatable recognition of cancer cells. The immunosensor was stable for three weeks and showed good precision with the relative standard deviation (RSD) of 3.57% and 2.12% assayed at the cell concentrations of $1.5x10^3$ and $1.5x10^5$ cells mL^{-1} respectively. The proposed single-wall carbon nanotube based immunosensor showed better analytical performance in comparison to similar leukemia electrochemical sensors reported.

Keywords: P-glycoprotein (P-gp); Fluorescence Microscopy; Electrochemical Sensor; Chronic Myeloid Leukemia; Single-wall Carbon Nanotube.

Introduction

Cancer is the second major cause of global mortality and also a leading cause for 8.8 million deaths in 2015 **[1]**. Leukemia, a malignancy of the early blood cells, mostly starts in the bone marrow and infiltrates in the blood. It is the most common cancer in children and teens, where it is acute or fast-growing in nature. In adults, leukemia is mostly chronic and slow growing. According to the American cancer society, leukemia is ranked 7^{th} in the estimated death rate in 2018 (24,370 people) and 10^{th} in the estimated new cases in 2018 (60,300 cases) **[2]**. Early

detection leads to a better disease outcome and therefore, has spurred the need for both biomarkers as well as improved technology **[3-5]**. Early, efficient, and specific detection of cancer are the key features that can determine the therapeutic regimen for a patient. Fabrication of biosensors for detection of low cancer cell count is now being done using nanomaterials that increase the surface area for maximum detection **[6]**. In this work, we have used P-glycoprotein (P-gp), a protein over expressed in drug resistant cells, responsible for pumping drugs out of the cells resulting in failure of chemotherapy treatment **[7-11].** Expressed on the cell surface, P-gp emerges as a good candidate for detection of difficult to treat cancers. In this paper, we show that P-gp expressing leukemia cells bind to its respective antibodies on the transducer surface, resulting in immune-complex formation; thereby, generating changes in the bioelectro-chemical signal in an electrochemical cell.

Different nanomaterials have been used for biosensors fabrication. Diverse nanomaterials successfully utilized as biosensors include gold nanoparticles, polymers, quantum dots, carbon nanoparticles and nanowires. Gold nanoparticles (AuNPs) have huge advantage in the field of bio-nanotechnology owing to their biocompatibility, diminished cytotoxicity, large surface area, good optical and electrical properties, although their high cost is a disadvantage **[12]**. The ability of AuNP to mediate electron transfer between the electroactive biological analyte and electrode reduces redox enzyme biosensing because a non-negligible amount of these molecules is lost in solution while diffusing to the electrode surface **[13]**. Quantum dots, a nanomaterial used widely in photo-electrochemical and optical sensing, also face challenges due to crystal lattice structural defects that trap electrons and holes leading to non-radiative relaxation **[14]**. Additionally, quantum dots require biocompatible coating on its surface to facilitate immobilization of biomolecules on it [**15**]. Magnetic nanoparticle a new entrant as a biosensor material forms a highly sensitive transducer not susceptible to any noise or interference while generating signals. However, immobilization of biomolecules requires a magnetic label to acquire signals, and an elaborate magnetic detection system [**16**, **17**]. Presently, carbon nanomaterials such as carbon nanotubes (CNTs)_and graphene are being extensively used for biosensing as electronic and electrochemical transducers [**18, 19**]. Particularly, CNT possesses molecular wire morphology with a unique combination of biocompatibility and electronic properties. They can be easily functionalized with organic molecules to provide attachment site for biomolecules and facilitate bio-electrochemical reactions **[20, 21]**. It has high surface area to volume ratio, thereby increases the sensitivity of the sensor. Furthermore, label free detection is possible based on the molecular recognition events **[22, 23]**.

Investigators have extensively explored various biosensor fabrications used for chronic myeloid leukemia (CML) detection. Immunoassay of leukemia K562 cells was carried out using glassy carbon electrode (GCE) modified either with AuNP/chitosan, or with cross-linker, could detect $8.71x10^2$ cells/mL and $1x10^4$ cells/mL cells, respectively [**24, 25**]. In 2007, Chen Hao fabricated electrochemical immunosensor using epoxy silane modified GCE and estimated a detection limit of $7.1x10^3$ cells/mL [**26**]. Complex genosensor and cytosensor fabrication based on GCE

modified with graphene sheets/chitosan solution or with AuNP-PANI nanofibers linked with anti-P-gp have also been used **[27, 28]**. GCE modifications with either platinum nanoparticles dotted CNT or with 3-aminophenylboronic acid functionalized manganese doped quantum dots cyto-sensors have detected 500 and 200 cells/mL respectively **[29, 30]**. Due to high stability of indium tin oxide (ITO) glass substrate, it has also been used as working electrode with certain modifications. Fabrication of electrochemical genosensors were established using composite of chitosan – cadmium telluride quantum dots and amine functionalized silica coated zinc oxides nanoparticles with estimated detection limit of 2.56 pM and $1x10^{-16}$ M concentration respectively **[31, 32]**. Chunmei Yu *et al* developed electrochemical immunosensor based on ITO with $1.2x10^{3}$ cells/mL detection limit **[33]**. Electrochemical impedance cyto-sensor was fabricated to detect leukemia K562 cells by assembling a biocompatible film of graphene oxide and poly-$_{L}$-lysine where an astounding detection of 30 cells/mL was reported [**34**]. An electro-chemiluminescence sensor, a disposable device for ultrasensitive detection of leukemia K562 cells, detected 46 cells/mL where screen printed electrode was modified with nano-porous gold, and carbon quantum dots coated ZnO nanosphere **[35**].

Various electrochemical based immunosensors, genosensors, cytosensors and aptamer- sensors have also been fabricated for cancer detection other than CML. Of these, carbon nanomaterial based biosensors have been reported with enhanced electrochemical performance. Carbon Nanotubes (CNTs) based label capable of dramatic signal amplification of nucleic acid detection of human acute lymphocytic leukemia (ALL) [**36**], immunosensor for detection of α-fetoprotein [**37**] and carcinoembryonic antigen [**38**], using AuNPs on CNTs have been constructed. Qin Shen *et al* fabricated electrochemical biosensor based on carbon paper, modified with TiO_2/CNT nanocomposites on which different drug resistant leukemia cells were recognized based on their different electrochemical behavior [**39**]. The electrochemical genosensor constructed for the detection of acute promyelocytic leukemia based on ordered FePt nanoparticles decorated CNTs, showed detection limit of $2.1x10^{-13}$ mol/L [**40**]. Electrical biosensors developed from CNT-Field Effect Transistor have been used for detection of prostate cancer marker (PSA-ACT complex) and immunoglobulin E (IgE) for allergy related disorders with detection limit of 1 ng/mL and 250pM respectively **[41, 42]**.

Multi-walled carbon nanotubes (MWCNTs) have also been used because of its high surface area to volume ratio, an attractive property for making efficient sensors. Ying Wan *et al* fabricated electrochemical immunosensor using HRP functionalized MWCNTs for cancer biomarkers detection such as prostate specific antigen and interleukin; and could detect 5 pg mL^{-1} and 8 pg mL^{-1} respectively [**43**]. With the aim of ultra-high sensitive microRNA (miRNA) electrochemical biosensor fabrication, MWCNTs-polyamidoamine (PAMAM) dendrimer modified GCE was synthesized and obtained 0.5 fM concentration detection limit **[44]**. Pencil graphite electrode modified with polypyrrole and functionalized with MWCNTs to detect 0.08 μmol L^{-1} concentration of 6-mercaptopurine (6-MP) [**45**]. There are reports on MWCNTs-ionic liquid electrode coated with AuNPs for breast cancer detection and Pb-ion based for

hepatocellular cancer detection with estimated detection limit of 7.4 ng mL^{-1} and 3.33fg/mL respectively [**46, 47]**.

Graphene has been utilized for fabricating biosensors owing to its extraordinary physical and chemical properties **[48]**. Unlike CNTs, graphene has the additional advantage to capture cancer cells on both side of the monolayer. Jiyang Liu *et al* demonstrated electrochemical immunosensor based on monolithic and macroporous graphene foam as a free standing three dimensional electrode for carcinoembryonic antigen detection and could detect 90 pg/mL cells concentration **[49]**. Graphene modified pencil graphite electrode were used for microRNA-21 detection [**50].** AuNP and toluidine blue based Graphene Oxide electrode have also been fabricated and the obtained detection limit was $2.95x10^{-12}$ M concentration [51].

In this manuscript, a novel immunosensor has been fabricated based on silicon (Si) wafer modified with single-wall carbon nanotubes (SWCNTs) followed by functionalization with 1% 3- glycidoxy-propyl-trimethoxy silane (3-GPMS) to hold antibody molecules on the electrode surface for electrochemical detection of the leukemia K562 cells. Cyclic Voltammetry (CV) and Electrochemical Impedance spectroscopy (EIS) studies were undertaken to acquire signal from the biosensor as biological signals are electrochemical in nature; therefore, electrochemical detection is a suitable technique. This method is convenient, fast, reliable, and cost-effective. The performance of the proposed sensor is found to be much superior in terms of crucial sensor parameters such as lower detection limit (LOD), reproducibility, repeatability, shelf-life and stability. The LOD obtained from the proposed sensor is 19 cells/mL. The SWCNT is found to be highly efficient in comparison to the other reported MWCNTs based biosensors due to its highly reactive sensor surface comprising of smaller diameter as compared to MWCNTs. Due to its molecular wire morphology, electron flow path becomes flawless which makes it an outstanding candidate for carrying out electrochemical sensing.

Reagents and Materials Required

3- Glycidoxy-propyl-trimethoxy silane, Monoclonal anti-P-glycoprotein antibodies, and Bovine Serum Albumin (BSA) were purchased from Sigma Aldrich, India. Trypan dye and RPMI-1640 media were procured from HiMedia, and Cell Clone respectively. Human Leukemia K562 cells were procured from National Centre for Cell Science (NCCS), Pune. The nuclear stain i.e. 4', 6-diamidino-2-phenylindole (DAPI) was purchased from Sigma Aldrich. Alexa Flour 488, and 4 well chamber slide were procured from Thermo Scientific and SPL Life Sciences Co., Ltd. respectively.

Synthesis of SWCNT/SiO_2/Si electrode

Synthesis of SWCNT was carried out using thermal chemical vapor deposition method. A Fe-Mo catalyst island of 0.5 nm thickness was co-sputtered on the SiO_2/Si substrate where Mo acts as a promoter to make carbon feedstock more active for CNT formation. Nucleation sites were

created by annealing the catalyst at 800°C in Ar/H_2 atmosphere for 30 min. Acetylene, 'the carbon feedstock' is flowed through the quartz tube for 3 min with the flow rate of 5 sccm at 775 degree Celsius which is the transition temperature of the metal nanoparticles to react with it to form the SWCNT. 60 torr growth pressure was maintained. High quality SWCNT network was synthesized with this method. One end of the electrode was sputtered with Au to make the electrical contact through which connection was developed.

Cell Culture

Human leukemia K562 cells were cultured in a T-75 cm^2 flask containing complete RPMI-1640 media with 10% fetal bovine serum and 10 µg mL^{-1} Ciprofloxacin in an incubator with 5% CO_2 at 37°C. Trypan blue dye exclusion method was utilized for cell counting using Neubauer's chamber with 10 µl of cell suspension mixed with 10 µl of dye. After a week on confluency, the cells were centrifuged at 1100 rpm for 10 min. The pellet obtained was washed twice with PBS and re-suspended in the sterile PBS buffer to prepare different dilutions from the stock which were used for sensing.

Assembly of Immunosensor

SWCNTs film developed on SiO_2/Si substrate was first exposed to O_2 plasma treatment for 15 min to make the surface hydrophilic in nature and then functionalized with 1% 3-GPMS in acetone for 18 h at room temperature. It acts as a necessary linker molecule to bind antibody to the electrode surface which is used for the detection of leukemia cells. After binding, the electrodes were washed with acetone to remove the physically adsorbed coupler molecules. Titer concentration in 1:500 ratio of anti-P-glycoprotein antibody (in PBS) was immobilized on the electrode surface for 24 h at 4°C and then washed with PBS (pH=7.4) to wipe out unbound antibody biomolecules. Here, highly reactive epoxy groups of the linker molecules readily react with $-NH_2$ group of the antibody to form the -CN covalent bond in order to prevent the leaching out of the bio-species during electrochemical sensing. Non-binding sites present on the surface of bio-electrodes ($Ab/Epoxy/SWNT/SiO_2/Si$) were blocked by 1 wt% BSA (in PBS). Incubation with BSA was carried out for 1 h at room temperature, followed by washing with PBS buffer. In the next step, the prepared bio-electrodes were incubated for 2 h at room temperature with different leukemia K562 cells concentration ($1.5x10^7$ to $1.5x10^3$ cells/mL) in PBS buffer (pH=7.4). Eventually, electrochemical sensing was done with these bio-electrodes to determine the binding effectiveness. The electrodes were stored in PBS at 4°C until their use in sensing. Scheme 1 shows the fabrication procedure of the proposed immunosensor.

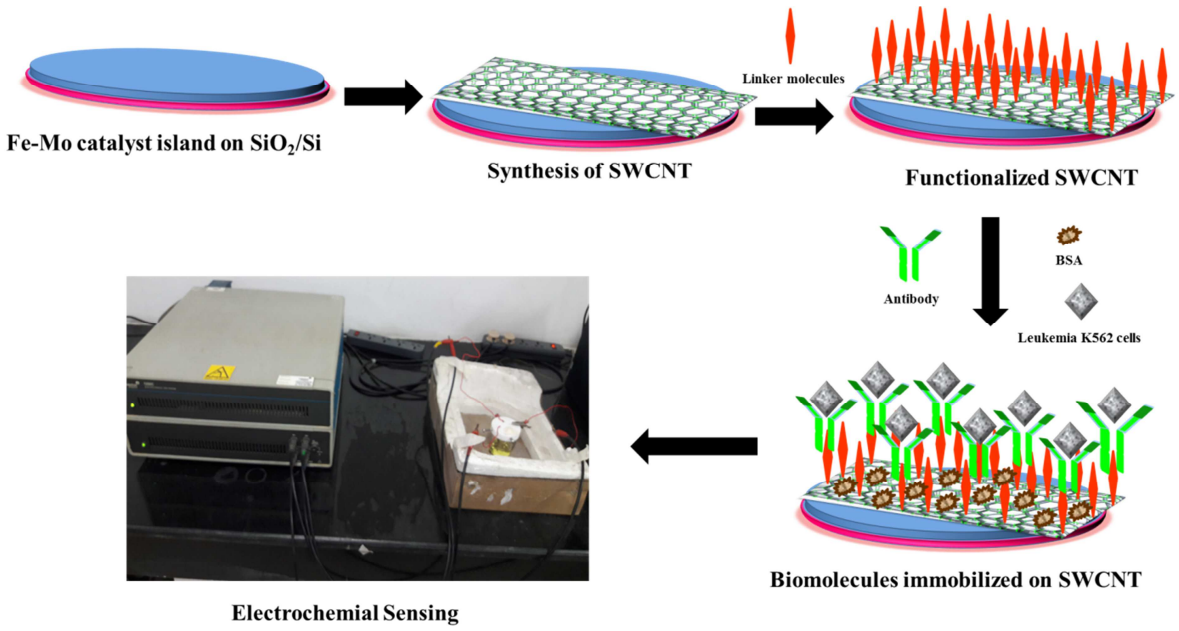

Scheme 1: Fabrication procedure of the proposed immunosensor

Characterization of the Electrochemical Biosensor

Cyclic Voltammetry (CV) is a potentio-dynamic electrochemical method which is used to study the resulting current change of the modified electrode surface in an electrochemical cell. CV was conducted on Solatron 1280 C Potentiostat/Galvenostat with conventional three electrode system in which Ag/AgCl was used as a reference electrode, platinum as counter electrode and SWCNT/SiO_2/Si as a working electrode. The alterations in the cathodic- anodic peak current and peak potentials of working electrode were studied using 5 mM concentration of redox mediators $K_3Fe(CN)_6$ / $K_4Fe(CN)_6$ in PBS buffer (pH=7.4) with potential range from -0.9 to +0.9 V at the scan rate of 50 mV/s. Additionally, electrochemical impedance spectroscopy(EIS) measurement was carried out in 5 mM of $K_3Fe(CN)_6$ / $K_4Fe(CN)_6$ and 0.1 M KCl (as electrolyte) in PBS (pH=7.4) in the frequency range of 1 MHz to 1 Hz keeping 5 mV amplitude of sine wave potential using Solatron electrochemical workstation (Modulab XM). FTIR (Vertex 70V, Bruker Optik) and Raman spectroscopy (LabRam HR800, JY) were used to measure the vibrational modes arisen due to attachment of different molecular species right from surface activation to immobilization process. Scanning Electron Microscope (Nova NanoSEM 450, FEI; and Sigma, Zeiss) were used to confirm the synthesis of the CNTs and attachment of biomolecules. The fluorescent microscope study was carried out on the Olympus IX83.

Expression analysis of P-gp by fluorescent microscopy

Expression of P-glycoprotein, present on the leukemia K562 cell surface, was determined by fluorescence microscopy. Immunofluorescence (IF) analysis is an influential technique for

visualizing intracellular processes, conditions and structures. It includes various steps and every step is followed by washing of cells with PBS for 5 min each. Firstly, media containing $1x10^7$cells/mL was added to the four-well chamber slide and subsequently, media was removed from the settled cells. Next step includes fixation, where cells were fixed in 4% paraformaldehyde for 5-10 min at room temperature. Thereafter, blocking was done with 3 wt% BSA for 1 h in order to minimize false positive signals from binding of antibodies to non-target structures. Further, in the first incubation step, cells were incubated with primary antibody in 1% BSA, and kept in humidified chamber at 4°C overnight. In the second incubation step, cells were then incubated with secondary antibody, Alexa Flour 488 (in 1% BSA) for 2 h at room temperature. Finally, a nuclear staining was done by adding 1 μg/mL DAPI in PBS for 5 min at room temperature. Then, cells were washed with PBS for 5 min and air dried. The cover slip was mounted with the drop of fluoroshield which is used to prevent quenching and sealed with the help of a transparent nail polish to prevent drying as well as movement under microscope.

Result and Discussion

Characterization of the SWCNTs

Scanning Electron Microscope (SEM) was used to study the surface morphology of the electrode. Raman spectroscopy (RS) was used to confirm the graphitic nature of single walled carbon nanotube, and Fourier Transform infrared (FTIR) spectroscopy was used to study the presence of surface functional groups.

In scanning electron micrograph [as shown in Fig 1(a)], it was clearly visible that CNTs are highly entangled to form an enormous network of SWCNTs. Nanotubes are randomly arranged in horizontal direction, densely packed and uniformly dispersed over the entire SiO_2 surface.

Raman spectroscopy is often used to characterize SWCNTs [**52**]. In Fig 1(b), peak at 210 cm^{-1} represents the presence of Radial Breathing Mode (RBM) which is characteristic of SWCNT and is diameter dependent [**53**]. The diameter calculated from the aforementioned RBM mode is ~1.18 nm **[53]**. The peak at 1345 cm^{-1} corresponds to the D-band where its intensity is used to ascertain the density of the defects present in the tube, whereas the band at 1587 cm^{-1} corresponds to G-band, characteristic of graphitic nature of the nanotube [**54**]. The 2D band which is sometimes also called as G' band is obtained at 2676 cm^{-1} arises due to two phonon resonance effect [**55**].

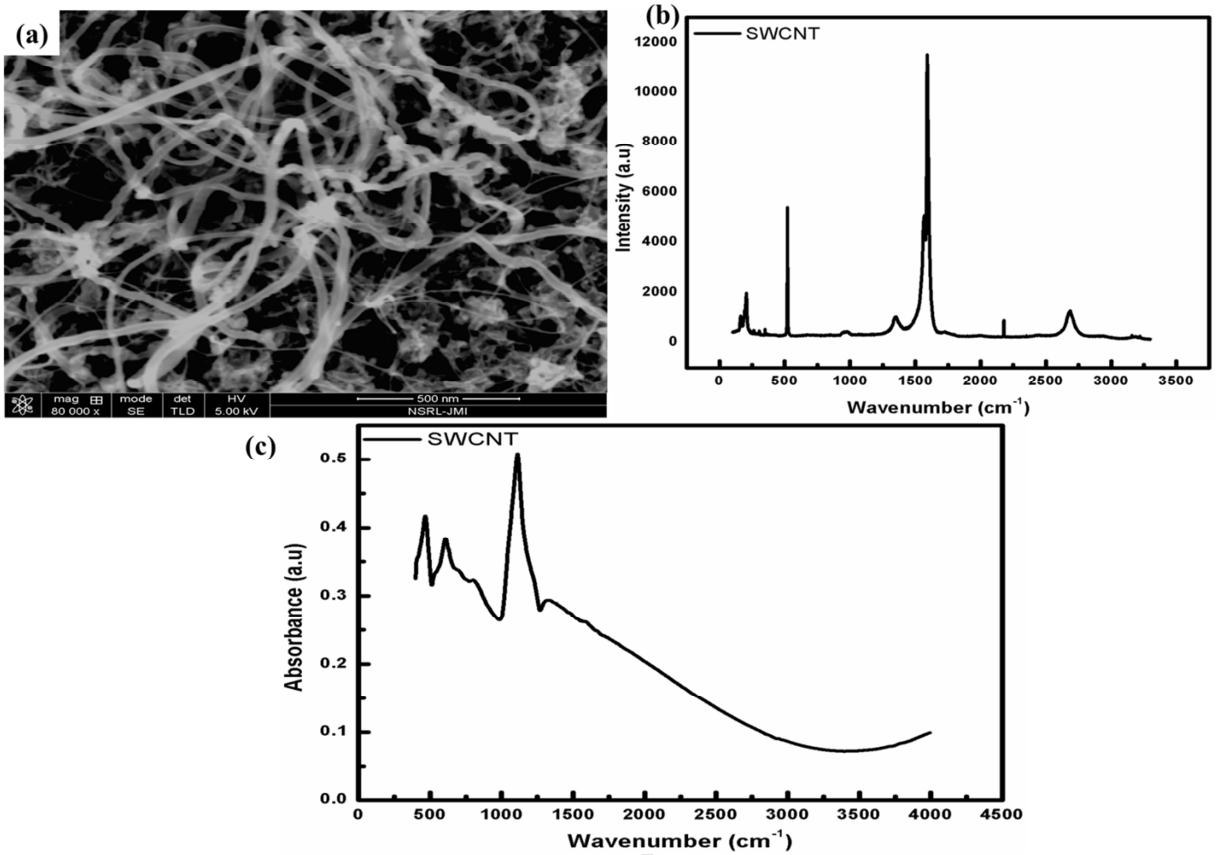

Fig 1: (a) SEM micrograph of SWCNT, (b) Raman spectrum of SWCNT, and (c) FTIR spectrum of SWCNT.

FTIR study [as shown in Fig.1(c)] was performed to study the functional groups present on the CNT surface in a range of 400 – 4000 cm^{-1}. The peak at 612 cm^{-1} depicts the bending of C-H bond which is present adjacent to the carbon-carbon triple bond [**56**]. The absorption peaks at 471 cm^{-1} and 1100 cm^{-1} corresponds to the triply degenerated bending and stretching tetrahedron (i.e SiO_2) vibration modes respectively [**57**]. The small shoulder peaks at 813 cm^{-1} and 1325 cm^{-1} represents the graphitic characteristic modes [**58**].

Characterization of the modified electrode

To confirm the immobilization of antibody and cells on the electrode surface, FTIR spectra and SEM images are given below.

The FTIR spectrum of antibody treated bio-electrode [as represented in Fig 2(a)] was similar to the carbon nanotube spectrum barring few different peaks which are mentioned in Table 1(a) below.

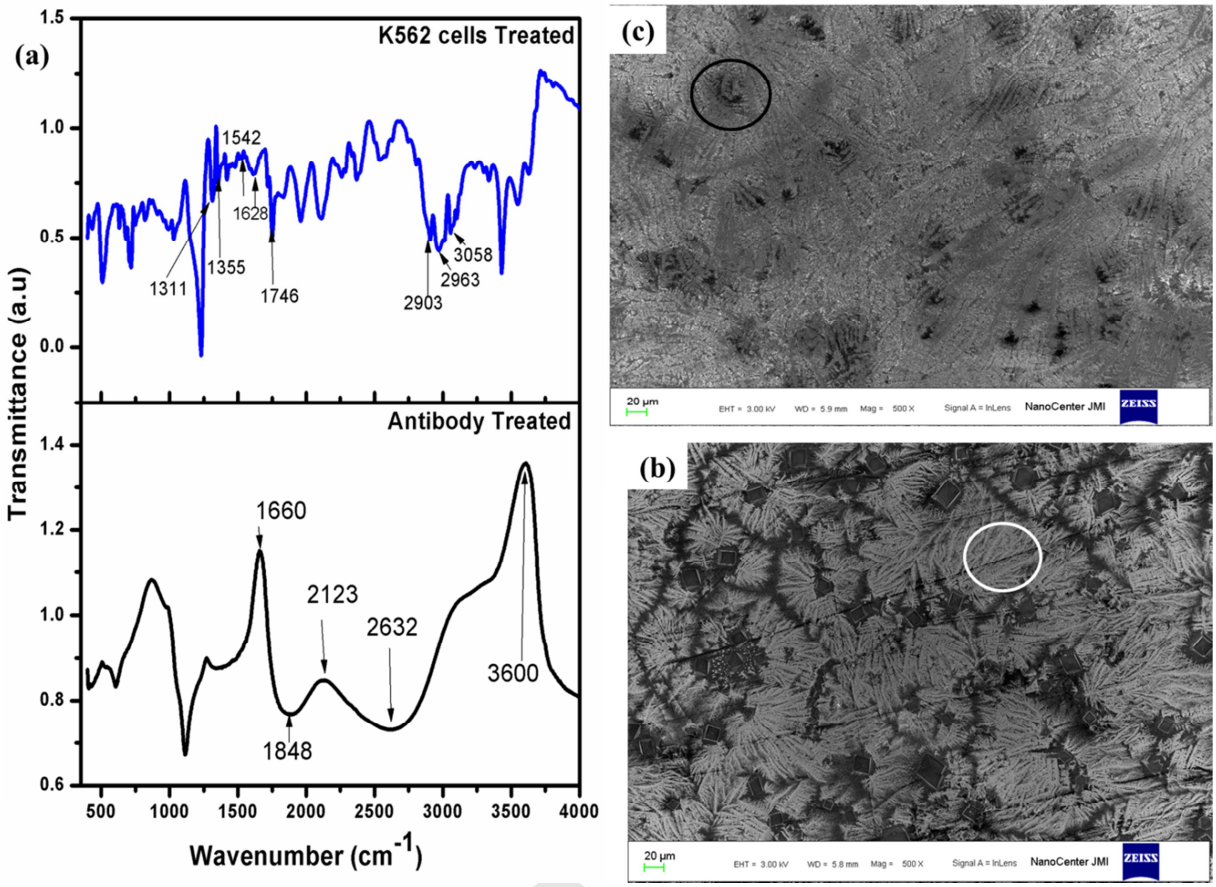

Fig 2: (a) FTIR spectra of anti-P-gp antibody and leukemia K562 cells treated bio-electrodes; FESEM images of (b) anti-P-gp antibody treated bio-electrode, (c) leukemia K562 cells treated bio-electrode.

Table 1(a): FTIR analysis of anti-P-gp antibody treated bio-electrode.

S.No.	Wavenumber (cm^{-1})	Assignment	Ref.
1	1660	Corresponds to amide bond	**59**
2	1848	Corresponds to lactones	**60**
3	2123	Corresponds to C≡C	**60**
4	2632	Corresponds to primary amine	**60**
5	3600	Corresponds to free - OH bond	**60**

The primary amine group confirmed the attachment of antibodies to the electrode surface as NH_2 group is present on the antigen binding site, Fab and Fc fragments of the antibody **[61, 62]**. The reaction involves (amide bond formation) primary amine of antibody with the epoxide group of silane molecules to form secondary amine and hydroxyl group as shown below [**63**]:

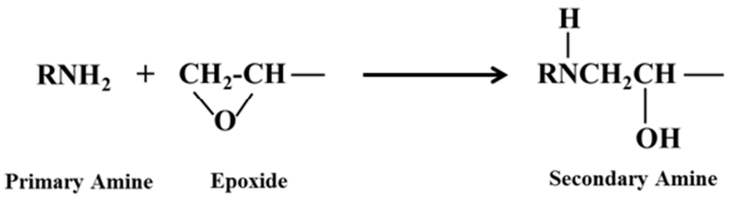

Lactones (-OCO-) and C≡C groups are present in the 3-glycidoxy-propyl-trimethoxy silane molecules.

Similarly, FTIR spectrum of leukemia K562 cells, immobilized on bio-electrode is represented in Fig (1a). The spectrum showed many peaks and few of them are listed in Table 1(b).

Table 1(b): FTIR analysis of leukemia K562 cells immobilized bio-electrode.

S.No.	Wavenumber (cm^{-1})	Assignment	Ref.
1	1311	Corresponds to amide III	**64**
2	1355	Corresponds to symmetric C-O and C-H stretching	**64**
3	1542	Corresponds to amide II stretching	**64**
4	1628	Corresponds to amide-I beta sheet	**64**
5	1746	Corresponds to C=O (lipids)	**64**
6	2903	Corresponds to asymmetric CH-CH_2 stretching of fatty acid	**64**
7	2963	Corresponds to symmetrical CH-CH_3 stretching of fatty acid	**64**
8	3058	Corresponds to amide A	**64**

These bonds confirm the attachment of leukemia cells to the electrode surface because cell membrane consists of proteins, carbohydrates and lipids. Amide I and amide II are indicative of the secondary structure of protein [**65**]. Amide III is also another characteristic band of protein which is ~ located at 1310 cm^{-1}. This region represents the PO_2 stretching mode of nucleic acid and the CO stretching vibrations from glycogen and carbohydrate residues [**66- 69**].

SEM images shown in Fig.2 (b & c) verified the attachment of antibodies and cells to the electrode surface. The coagulation of anti-P-gp antibodies (circled white) in Fig 2(b) confirmed their attachment all over the electrode surface. In Fig 2(c), leukemia K562 cells (circled black) confirmed their attachment to the antibody molecules resulting in immune-complex formation. Due to non-conducting nature of cells, charge carrier (electrons) transfer between the electrode and the immobilized analytes were prevented. This non-conducting nature was confirmed by charging phenomenon on the electrode surface during sample scanning and it is more wherever cells are bound.

Electrochemical Characterization of the modified electrodes

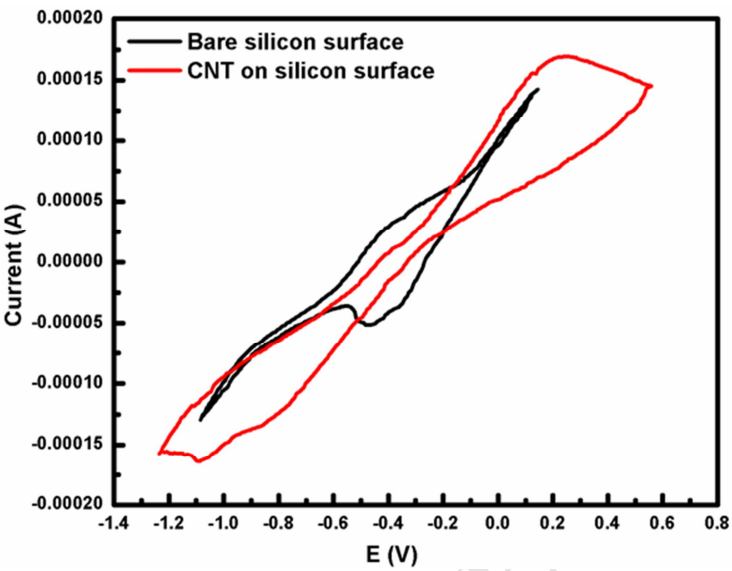

Fig 3: Cyclic voltammogram of bare (black) and SWCNT modified (red) Si wafer.

The characteristics of the modified electrode were analyzed with the help of CV spectra as shown in Fig 3. The figure shows that CNT synthesis resulted in enhanced redox activity on the electrode surface. The nanotube clearly acts as a conducting path facilitating electron transport on an enlarged surface area where all the sensing atoms are present on the tube surface. The larger effective surface area provided by SWCNT was validated by observing the increased anodic/ cathodic peak current and position of redox waves. SiO_2 provided good adhesive strength to the CNTs deposited on the Si substrate, was evident from the inhibited leaching out of the CNT film from the wafer surface during experiment. CNT electrode was highly stable as observed by the repetitive and overlapping loops of redox peak current obtained in multiple cycles (not shown). The increased redox current in CV measurements of SWCNT/Fe-Mo/SiO_2/Si surface is considered for charge capacitance of inner and outer surface of CNTs.

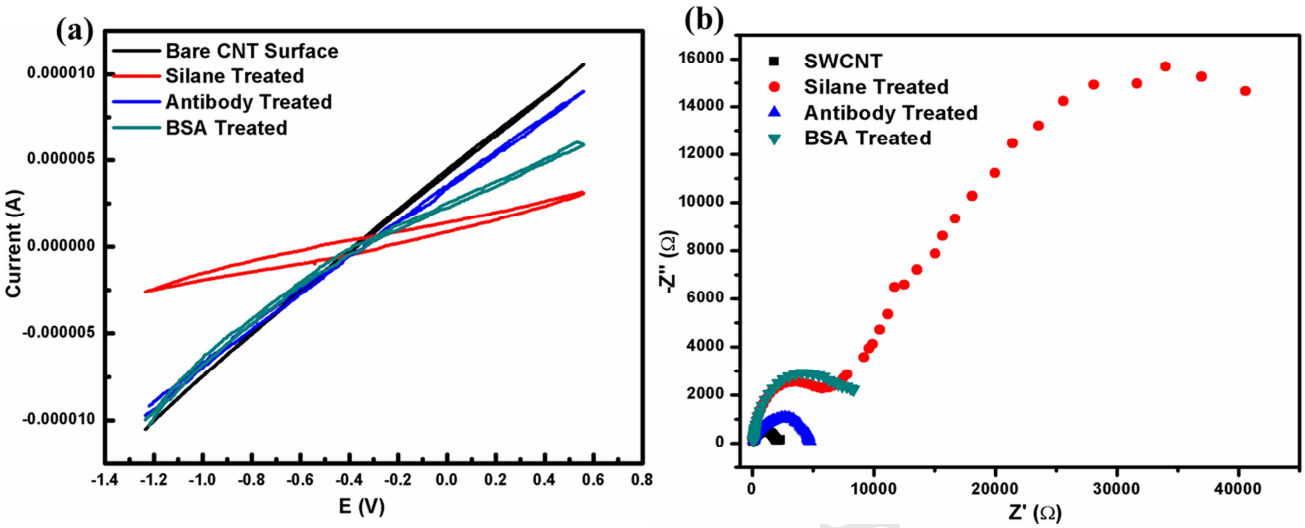

Fig 4 (a) Cyclic voltammogram of modified bio-electrodes: bare nanotube surface, black; silane treated surface, red; antibody immobilized, blue; BSA immobilized, dark cyan. (b) Impedance spectra of modified bio-electrodes: bare nanotube surface, black; silane treated surface, red; antibody immobilized, blue; BSA immobilized, dark cyan.

When CNT was functionalized with the linker molecules [Fig 4(a)], the anodic peak current dropped significantly due to epoxy group which acts as an insulator and thus preventing the flow of electron transport on the electrode surface. Additionally, as a consequence of covalent functionalization in SWCNT, few C=C double bond were broken while leaving behind holes in the nanotube thus, render to alter the electrical properties. Further, on immobilizing anti-P-gp biomolecules the peak current was increased possibly due to the lone pair of electrons present on the N of the NH_2 group of an antibody biomolecule. Subsequently when non-active sites of the electrode were blocked with the BSA, there was, again a slight fall in the peak current that can be attributed to the blockage of mass transfer of electrons due to the bulky protein groups. The impedance plot [Fig 4(b)] shows that after silane treatment on the SWCNTs, resistance increased significantly (R_{et}= 40,573 Ω) vis-à-vis the nanotubes resistance (R_{et}= 2298 Ω). This is attributed to the fact that nanotubes got wrapped with the insulating linker molecules. Further when antibody immobilization was done to the electrode surface the resistance value decreased (R_{et}= 4690 Ω) because electrons were donated by the lone pair of nitrogen atom. Thereafter, resistance value again increased (R_{et}= 8336 Ω) due to bulky protein molecules (i.e. BSA) used to block non-target sites. The results were found to be in good agreement with Fig 4(a) showing cyclic voltammogram of modified bio-electrodes.

Before detecting the expression of P-gp electrochemically, the leukemia K562 cells were first checked for P-gp expression on their surface. For this, immunofluorescence analysis was done.

Expression analysis of target protein p-gp on K562 cell surface

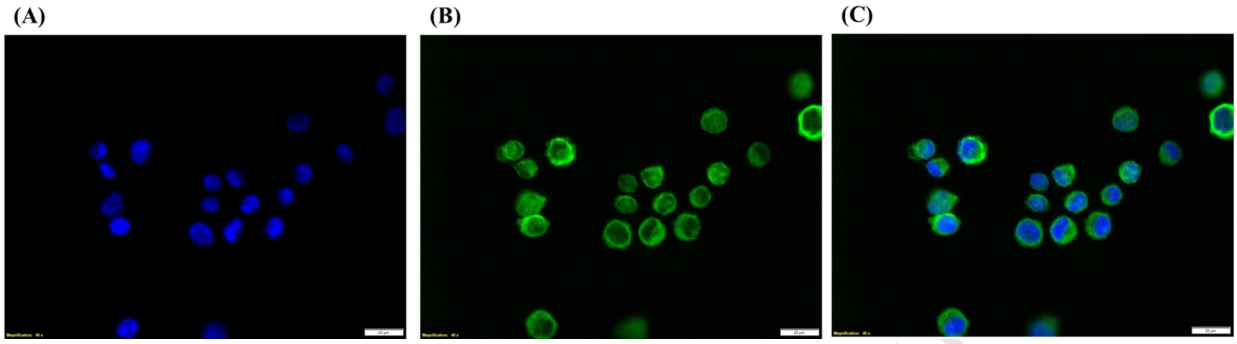

Fig 5: Fluorescence micrographs showing (a) DAPI stained DNA, (b) Alexa-fluor 488 stained P-gp transporters, (c) merged image of a & b showing maximal localization of P-gp on cell surface.

Fig 5(a) depicts the staining of the nuclear DNA performed with the help of DAPI dye [**70**]. These dye molecules intercalate with the DNA thereby marking the nucleus of a cell. Fig 5(b) shows the stained P-gp transporters (through secondary antibodies named Alexa Flour 488) present on the surface of the leukemia cells **[71]**. Fig 5(c) confirms the presence of transporters on the leukemia K562 cell surface.

Cyclic voltammetry measurement for leukemia K562 cell detection

Another interesting feature of the proposed biosensor was observed in its sensing performance. When the concentration of the leukemia cells was increased the peak current decreased for the same [Fig 6(a)] due to the insulating nature of these cells [**72-74**]. These results implicate that bulkier cells prevent the flow of electrons through the conducting nanotube. A larger surface area of SWCNT can provide more active sites for biomolecules attachment therefore, making the sensor more sensitive. Fig 6(b) shows the linear calibration plot (peak current v/s the logarithm of concentration of leukemia K562 cells) with a regression coefficient of 0.935 for $1.5x10^3$ to $1.5x10^7$ cells/mL concentration range and detection limit was found to be 19 cells mL^{-1} [**75**]. Cyclic voltammetry is highly sensitive technique as it can compute extremely low detection limit [**76**]. The peak current of non-faradic current in cyclic voltammetry experiment appears to be the hysteresis current given by the equation [**77**]:

I_{nF} = (Ia-Ic/2) where Ia stands for anodic peak current and Ic for cathodic peak current.

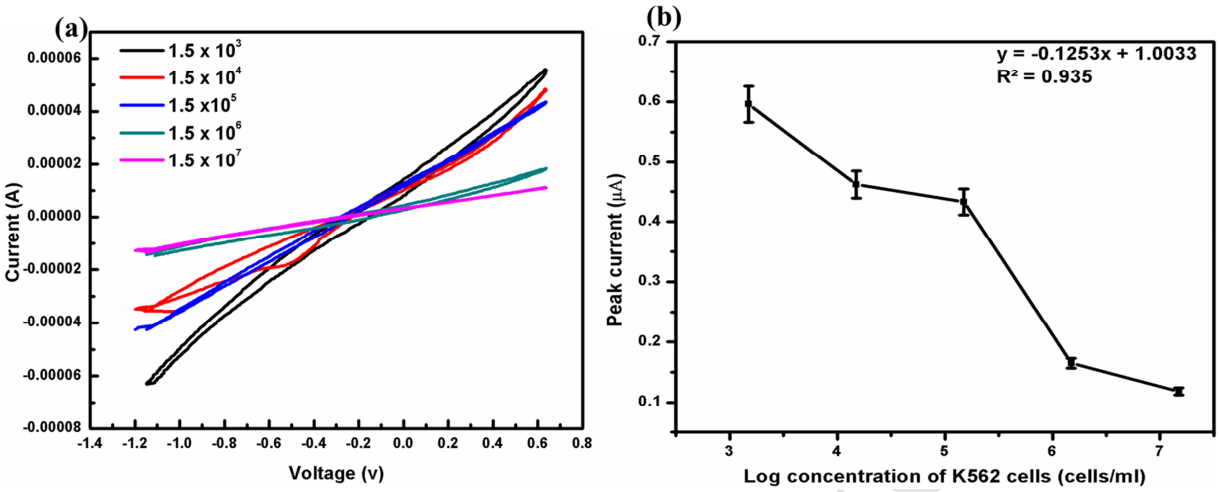

Fig 6: (a) Cyclic voltammogram of fabricated immunosenor at different cell concentrations: $1.5x10^7$, $1.5x10^6$, $1.5x10^5$, $1.5x10^4$, $1.5x10^3$cells/mL; (b) Calibration plot: peak current v/s logarithm of concentration of K562 cells.

The experimental detection limit as obtained from the calibration plot (Fig 6b) was calculated using the following equation:

LOD [**8**] = K x (S.D) / S

where,

K = 3.3, the confidence level parameter which is related to noise with statistical confidence of 99%.

S.D = Standard deviation of blank measurements (for 3 measurements).

S = Slope of calibration plot (peak current v/s logarithm of concentration of K562 cells).

The comparison of sensitivity/LOD of our fabricated immunosensor with other existing sensors for CML detection is shown in Table 2.

Table 2: Comparison of sensitivity/LOD of fabricated immunosensor with other existing sensors for CML detection.

Nanomaterial modified electrode	Sensing	Sensitivity/ LOD	Ref.
AuNPs / GCE	Electrochemical	$1x10^4$ cells/mL	24
AuNP's-chitosin modified GCE	Electrochemical	$8.71x10^2$ cells/mL	25
GCE	Electrochemical	$7.1x10^3$ cells/mL	26
Graphene sheets/chitosan/GCE	Electrochemical	2.11 pM	27
AuNP-PANI nanofibers	Electrochemical	80 cells/mL	28
Pt nanoparticles dotted CNT	Electro-chemiluminescent (ECL)	500 cells/mL	29
Mn doped quantum dots / GCE	Photo-electrochemical	200 cells/mL	30
Chitosan – cadmium telluride quantum dots / ITO substrate	Electrochemical	2.56 pM	31
Silica coated zinc oxides nano particles/ ITO	Electrochemical	$1x10^{-16}$ M	32
ITO	Electrochemical	$1.2x10^3$ cells/mL	33
Graphene oxide and poly-$_L$-lysine	Electrochemical	30cells/mL	34
Screen printed electrode/nano porous Au/ carbon quantum dots (CQDs) coated ZnO nanosphere	ECL	46 cells/mL	35
SWCNT/Si	Electrochemical	19 cells/mL	Present work

Electrochemical Impedance Spectroscopy (EIS) for detection of K562 cells

Fig 7(a) represents the Nyquist plot of EIS for SWCNT/Si modified surface on incubating with different concentrations of K562 cells. EIS measures the response by computing the impedance at each (low or high) frequency which equals the resistance value as depicted with a semi-circle. This response can be calculated through equivalent circuit (a network of circuit elements in an electrochemical cell). The circuit, shown in Fig 7(b), suitably fits the experimental data acquired throughout the frequency range (verified by ZSimpWin 3.21 software) and includes the following components: electrolyte resistance (R_s), charge transfer resistance (R_{ct}), electrode-electrolyte double layer capacitance (C_{dl}) and diffusion control for thin films (o) [**79**]. Fig 7(a) shows that the increase in charge transfer resistance (R_{ct}) with the confluence of cells on the transducer surface. Fig. 6 (a) and Fig. 7 (a) share similar observations of a significant increase in resistance or fall in current when the cell concentration reaches 1.5 million cells/mL and results are in good agreement with each other.

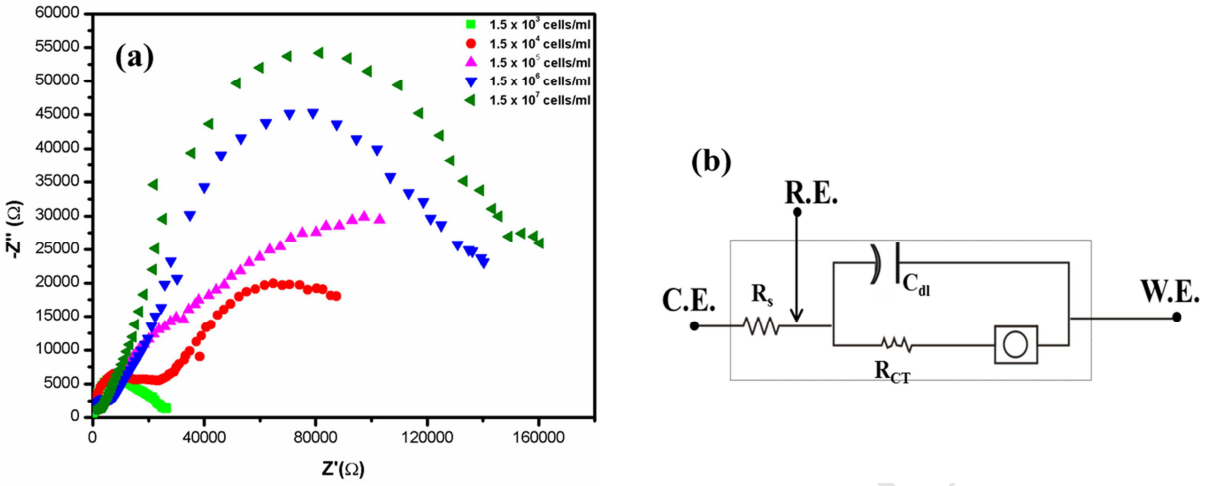

Fig 7: (a) Electrochemical Impedance spectra of fabricated immunosenor at different cells concentration: $1.5x10^7$, $1.5x10^6$, $1.5x10^5$, $1.5x10^4$, $1.5x10^3$ cells/mL; (b) equivalent circuit of the designed immunosensor.

Reproducibility of the biosensor

We have investigated the reproducibility of our biosensor using statistical analysis over a period of time. The immunosensor property was assessed with the intra-assay precision by calculating two different cells concentration values ($1.5x10^3$ and $1.5x10^5$ cells mL^{-1}); the relative standard deviation for 5 cyclic voltammetry measurements were found to be 5.57% and 3.68% respectively. To determine the long-term stability of the immunosensor, successive CV measurements were carried out. The relative standard deviation (RSD) obtained for 40 cycles of $1.5x10^3$ cells mL^{-1} and $1.5x10^5$ cells mL^{-1} range was 3.57% and 2.12% respectively. This indicates the good stability of the immunosensor where antibody modified SWCNTs provide strong immobilization capability to the leukemia K562 cells.

After three weeks, there was no apparent change in the CV readings for both the cell concentrations. The response of the fabricated immunosensor for the concentrations of $1.5x10^3$ and $1.5x10^5$ cells mL^{-1} was retained up to 95% and 93% respectively of its initial value. This indicates good stability of the sensor and assures that all modifications (Leukemia K562/P-gp/GPMS/SWCNT/Si) performed, get firmly attached to the electrode surface. Thus, the proposed method is successful for the fabrication of SWCNTs based immunosensors. Thus, we can conclude that electrochemical method provides good reproducibility and high stability as well as sensitivity.

Conclusion

A label-free cytosensor device based on electrochemical sensing for leukemia K562 cell detection is presented in this work. The use of single-wall carbon nanotube (SWCNT) electrode provides a biocompatible and highly sensitive platform for the chronic myeloid leukemia (CML)

detection with a lower detection limit of 19 cells/mL. The fabricated device is cheap and less time consuming in comparison with the available conventional techniques. The performance of the proposed immunosensor is found to be much superior to others in terms of the crucial sensor parameters such as LOD, reproducibility, shelf-life, and stability. The SWCNT is found even to be highly efficient in comparison to the other reported multi-wall nanotube based biosensors as the surface area becomes much larger in comparison to the later. Due to its smaller diameter, the curvature of the tube surface becomes stronger leading to more reactivity as well as high sensitivity. Therefore, SWCNT based electrode is preferred over MWCNT in developing immunosensor for CML detection.

References:

[1] World Health Organization, http://www.who.int/news-room/fact-sheets/detail/cancer (Accessed 12 June 2018).

[2] American Cancer Society https://cancerstatisticscenter.cancer.org/?_ga=2.210845333.1075551730.1528789954-1098326013.1460395245#!/ (Accessed 12 June 2018).

[3] Kumar, S., A. Mohan, and R. Guleria. "Biomarkers in cancer screening, research and detection: present and future: a review." Biomarkers 11.5 (2006): 385-405.

[4] Hanash, Samir M., Sharon J. Pitteri, and Vitor M. Faca. "Mining the plasma proteome for cancer biomarkers." Nature 452.7187 (2008): 571-579.

[5] D'haeseleer, Patrik. "How does DNA sequence motif discovery work?." Nature biotechnology 24.8 (2006): 959-961.

[6] Choi, Young-Eun, Ju-Won Kwak, and Joon Won Park. "Nanotechnology for early cancer detection." Sensors 10.1 (2010): 428-455.

[7] https://en.wikipedia.org/wiki/P-glycoprotein

[8] Eckford, Paul DW, and Frances J. Sharom. "ABC efflux pump-based resistance to chemotherapy drugs." Chemical reviews 109.7 (2009): 2989-3011.

[9] F. J. Sharom, “The P-glycoproteinmultidrug transporter,” Essays in Biochemistry, vol. 50, no. 1, pp. 161–178, 2011.

[10] Oswald, Christine, I. Barry Holland, and Lutz Schmitt. "The motor domains of ABC-transporters." Naunyn-Schmiedeberg's archives of pharmacology 372.6 (2006): 385-399.

[11] Germann, U. A. "P-glycoprotein—a mediator of multidrug resistance in tumour cells." European journal of cancer 32.6 (1996): 927-944.

[12] Connor, Ellen E., et al. "Gold nanoparticles are taken up by human cells but do not cause acute cytotoxicity." Small 1.3 (2005): 325-327.

[13] Holzinger, Michael, Alan Le Goff, and Serge Cosnier. "Nanomaterials for biosensing applications: a review." Frontiers in chemistry 2 (2014): 63-63.

[14] Murphy, Catherine J. "Peer reviewed: optical sensing with quantum dots." (2002): 520-A.

[15] Biju, Vasudevanpillai, Tamitake Itoh, and Mitsuru Ishikawa. "Delivering quantum dots to cells: bioconjugated quantum dots for targeted and nonspecific extracellular and intracellular imaging." Chemical Society Reviews 39.8 (2010): 3031-3056.

[16] Tamanaha, C. R., et al. "Magnetic labeling, detection, and system integration." Biosensors and Bioelectronics 24.1 (2008): 1-13.

[17] Liébana, Susana, et al. "Magneto immunoseparation of pathogenic bacteria and electrochemical magneto genosensing of the double-tagged amplicon." Analytical chemistry 81.14 (2009): 5812-5820.

[18] Vamvakaki, Vicky, and Nikos A. Chaniotakis. "Carbon nanostructures as transducers in biosensors." Sensors and Actuators B: Chemical 126.1 (2007): 193-197.

[19] Valentini, F., M. Carbone, and G. Palleschi. "Carbon nanostructured materials for applications in nano-medicine, cultural heritage, and electrochemical biosensors." Analytical and bioanalytical chemistry 405.2-3 (2013): 451-465.

[20] Ali-Boucetta, Hanene, and Kostas Kostarelos. "Carbon nanotubes in medicine & biology—Therapy and diagnostics." Adv. Drug Deliv. Rev 65 (2013): 1897-1898.

[21] Ménard-Moyon, Cécilia, et al. "Functionalized carbon nanotubes for probing and modulating molecular functions." Chemistry & biology 17.2 (2010): 107-115.

[22] Wang, Joseph. "Carbon-nanotube based electrochemical biosensors: A review." Electroanalysis 17.1 (2005): 7-14.

[23] Le Goff, Alan, Michael Holzinger, and Serge Cosnier. "Enzymatic biosensors based on SWCNT-conducting polymer electrodes." Analyst 136.7 (2011): 1279-1287.

[24] Du, Dan, et al. "Electrochemical immunoassay of membrane P-glycoprotein by immobilization of cells on gold nanoparticles modified on a methoxysilyl-terminated butyrylchitosan matrix." Biochemistry 44.34 (2005): 11539-11545.

[25] Ding, Lin, et al. "A bio-inspired support of gold nanoparticles− chitosan nanocomposites gel for immobilization and electrochemical study of K562 Leukemia cells." Biomacromolecules 8.4 (2007): 1341-1346.

[26] Hao, Chen, et al. "A self-assembled monolayer based electrochemical immunosensor for detection of leukemia K562A cells." Electrochemistry communications 9.6 (2007): 1359-1364.

[27] Wang, Li, et al. "Graphene sheets, polyaniline and AuNPs based DNA sensor for electrochemical determination of BCR/ABL fusion gene with functional hairpin probe." Biosensors and Bioelectronics 51 (2014): 201-207.

[28] Zhang, Shaolian, et al. "An efficient nanomaterial-based electrochemical biosensor for sensitive recognition of drug-resistant leukemia cells." Analyst 139.14 (2014): 3629-3635.

[29] Ge, Lei, et al. "Application of Au cage/Ru (bpy) 3 2+ nanostructures for the electrochemiluminescence detection of K562 cancer cells based on aptamer." Sensors and Actuators B: Chemical 214 (2015): 144-151.

[30] Wu, Peng, et al. "Long-Lived Charge Carriers in Mn-Doped CdS Quantum Dots for Photoelectrochemical Cytosensing." Chemistry-A European Journal 21.13 (2015): 5129-5135.

[31] Sharma, Aditya, et al. "Chitosan encapsulated quantum dots platform for leukemia detection." Biosensors and Bioelectronics 38.1 (2012): 107-113.

[32] Pandey, Chandra Mouli, et al. "Controlled deposition of functionalized silica coated zinc oxide nano-assemblies at the air/water interface for blood cancer detection." Analytica chimica acta 937 (2016): 29-38.

[33] Yu, Chunmei, et al. "A new disposable electrode for electrochemical study of leukemia K562 cells and anticancer drug sensitivity test." Biosensors and Bioelectronics 53 (2014): 142-147.

[34] Zhang, Dongdong, et al. "Graphene oxide/poly-l-lysine assembled layer for adhesion and electrochemical impedance detection of leukemia K562 cancer cells." Biosensors and Bioelectronics 42 (2013): 112-118.

[35] Zhang, Meng, et al. "A disposable electrochemiluminescence device for ultrasensitive monitoring of K562 leukemia cells based on aptamers and ZnO@ carbon quantum dots." Biosensors and Bioelectronics 49 (2013): 79-85.

[36] A.C. Lee, J.S. Ye, S.N. Tan, D.P. Poenar, F.S. Sheu, C.K. Heng, T.M. Lim, Carbon nanotube-based labels for highly sensitive colorimetric and aggregation-based visual detection of nucleic acids. Nanotechnology 18 (2007) 455102-455111.

[37] J. Lin, C. He, L. Zhang, S. Zhang, Sensitive amperometric immunosensor for α-fetoprotein based on carbon nanotube/gold nanoparticle doped chitosan film. Analytical biochemistry 384 (2009) 130-135.

[38] X. Gao, Y. Zhang, H. Chen, Z. Chen, X. Lin, Amperometric immunosensor for carcinoembryonic antigen detection with carbon nanotube-based film decorated with gold nanoclusters. Analytical biochemistry 414 (2011) 70-76.

[39] Q. Shen, S.K. You, S.G. Park, H. Jiang, D. Guo, B. Chen, X. Wang, Electrochemical biosensing for cancer cells based on TiO_2/CNT nanocomposites modified electrodes. Electroanalysis. 20 (2008) 2526-2530.

[40] W. Zhang, P. Zong, X. Zheng, L. Wang, An enhanced sensing platform for ultrasensitive impedimetric detection of target genes based on ordered FePt nanoparticles decorated carbonnanotubes. Biosensors and Bioelectronics 42 (2013) 481-485.

[41] J.P. Kim, B.Y. Lee, J. Lee, S. Hong, S.J. Sim, Enhancement of sensitivity and specificity by surface modification of carbon nanotubes in diagnosis of prostate cancer based on carbon nanotube field effect transistors. Biosensors and Bioelectronics 24 (2009) 3372-3378.

[42] K. Maehashi, T. Katsura, K. Kerman, Y. Takamura, K. Matsumoto, E. Tamiya, Label-free protein biosensor based on aptamer-modified carbon nanotube field-effect transistors. Analytical Chemistry 79 (2007) 782-787.

[43] Y. Wan, W. Deng, Y. Su, X. Zhu, C. Peng, H. Hu, H. Peng, S. Song, C. Fan, Carbon nanotube-based ultrasensitive multiplexing electrochemical immunosensor for cancer biomarkers. Biosensors and Bioelectronics 30 (2011) 93-99.

[44] F. Li, J. Peng, Q. Zheng, X. Guo, H. Tang, S. Yao, Carbon nanotube-polyamidoamine dendrimer hybrid-modified electrodes for highly sensitive electrochemical detection of microRNA24. Analytical chemistry 87 (2015) 4806-4813.

[45] H. Karimi-Maleh, F. Tahernejad-Javazmi, N. Atar, M.L. Yola, V.K. Gupta, A.A. Ensafi, A novel DNA biosensor based on a pencil graphite electrode modified with polypyrrole/functionalized multiwalled carbon nanotubes for determination of 6-mercaptopurine anticancer drug. Industrial & Engineering Chemistry Research 54 (2015) 3634-3639.

[46] Arkan, Elham, et al. "A novel antibody–antigen based impedimetric immunosensor for low level detection of HER2 in serum samples of breast cancer patients via modification of a gold nanoparticles decorated multiwall carbon nanotube-ionic liquid electrode." Analytica chimica acta 874 (2015): 66-74.

[47] Li, Faying, et al. "An ultrasensitive sandwich-type electrochemical immunosensor based on signal amplification strategy of gold nanoparticles functionalized magnetic multi-walled carbon nanotubes loaded with lead ions." Biosensors and Bioelectronics 68 (2015): 626-632.

[48] H.S. Wong, D. Akinwande, Carbon nanotube and graphene device physics, first edition, Cambridge University Press, New York, 2011.

[49] J. Liu, J. Wang, T. Wang, D. Li, F. Xi, J. Wang, E. Wang, Three-dimensional electrochemical immunosensor for sensitive detection of carcinoembryonic antigen based on monolithic and macroporous graphene foam. Biosensors and Bioelectronics 65 (2015) 281-286.

[50] Kilic, Tugba, et al. "Electrochemical Detection of a Cancer Biomarker mir-21 in Cell Lysates Using Graphene Modified Sensors." Electroanalysis 27.2 (2015): 317-326.

[51] Peng, Hua-Ping, et al. "Label-free electrochemical DNA biosensor for rapid detection of mutidrug resistance gene based on Au nanoparticles/toluidine blue–graphene oxide nanocomposites." Sensors and Actuators B: Chemical 207 (2015): 269-276.

[52] Reich, Stephanie, Christian Thomsen, and Janina Maultzsch. Carbon nanotubes: basic concepts and physical properties. John Wiley & Sons, 2008.

[53] Hennrich, Frank, et al. "Raman spectroscopy of individual single-walled carbon nanotubes from various sources." The Journal of Physical Chemistry B 109.21 (2005): 10567-10573.

[54] Thomsen, C., and S. Reich. "Double resonant Raman scattering in graphite." Physical review letters 85.24 (2000): 5214.

[55] Souza Filho, A. G., et al. "Anomalous two-peak G′-band Raman effect in one isolated single-wall carbon nanotube." Physical Review B 65.8 (2002): 085417.

[56] Silverstein, Robert M., et al. Spectrometric identification of organic compounds. John wiley & sons, 2014.

[57] Salh, Roushdey. "Defect related luminescence in silicon dioxide network: a review." Crystalline Silicon-Properties and Uses. InTech, 2011.

[58] Branca, C., et al. "Characterization of carbon nanotubes by TEM and infrared spectroscopy." The Journal of Physical Chemistry B 108.11 (2004): 3469-3473.

[59] Slide share https://www.slideshare.net/yousufzaidi/4424-structure-determination-through-ir (Accessed 15 May 2018)

[60] R.M. Silverstein, F.X. Webster, D.J. Kiemle, Spectrometric Identification of Organic Compounds, seventh ed., John Wiley & Sons, INC. New York, 2005.

[61] Thermo Fisher Scientific

https://www.thermofisher.com/in/en/home/life-science/antibodies/antibodies-learning-center/antibodies-resource-library/antibody-methods/antibody-fragmentation.html (accessed 9 April 2018).

[62] A. Makaraviciute, A. Ramanaviciene, Site-directed antibody immobilization techniques for immunosensors, Biosensors and Bioelectronics 50 (2013) 460-471.

[63] L. Shechter, J. Wynstra, R.P. Kurkjy, Glycidyl ether reactions with amines, Industrial & Engineering Chemistry 48 (1956) 94-97.

[64] L.B. Mostaço-Guidolin, L. Bachmann, Application of FTIR spectroscopy for identification of blood and leukemia biomarkers: A review over the past 15 years. Applied Spectroscopy Reviews 46 (2011) 388-404.

[65] H.H. Mantsch, D.Chapman, Infrared spectroscopy of biomolecules, first ed., Wiley-Liss. New York, 1996.

[66] H. Torii, M. Tasumi, H. Mantsch, D. Chapman, Infrared Spectroscopy of Biomolecules. Wiley-Liss, New York, (1996) 1-8.

[67] A. Bath, C. Zscherp, What vibrations tell about proteins. Q. Rev. Biophys. 35 (2002) 369-430.

[68] B.R. Wood, M.A. Quinn, B. Tait, M. Ashdown, T. Hislop, M. Romeo, D. McNaughton, FTIR microspectroscopic study of cell types and potential confounding variables in screening for cervical malignancies. Biospectroscopy 4 (1998) 75-91.

[69] M.A. Cohenford, T.A. Godwin, F. Cahn, P. Bhandare, T.A. Caputo, B. Rigas, Infrared spectroscopy of normal and abnormal cervical smears: evaluation by principal component analysis. Gynecologic oncology 66 (1997) 59-65.

[70] https://en.wikipedia.org/wiki/DAPI (Accessed 7 November 2017).

[71] Wojtal, Kacper A., et al. "Efficient trafficking of MDR1/P-glycoprotein to apical canalicular plasma membranes in HepG2 cells requires PKA-RIIα anchoring and glucosylceramide." Molecular biology of the cell 17.8 (2006): 3638-3650.

[72] Yang, Liju, Yanbin Li, and Gisela F. Erf. "Interdigitated Array Microelectrode-Based Electrochemical Impedance Immunosensor for Detection of Escherichia c oli O157: H7." Analytical chemistry 76.4 (2004): 1107-1113.

[73] Tlili, Chaker, et al. "Fibroblast cells: a sensing bio-element for glucose detection by impedance spectroscopy." Analytical chemistry 75.14 (2003): 3340-3344.

[74] Guo, Manli, et al. "Monitoring of cell growth and assessment of cytotoxicity using electrochemical impedance spectroscopy." Biochimica et Biophysica Acta (BBA)-General Subjects 1760.3 (2006): 432-439.

[75] Waldo, Albert L., and Gerard A. Kaiser. "A study of ventricular arrhythmias associated with acute myocardial infarction in the canine heart." Circulation 47.6 (1973): 1222-1228.

[76] www.hep.fsu.edu/~wahl/phy3091/sp05/talk3/RDiltzTalk3.ppt

[77] https://web.nmsu.edu/~snsm/classes/chem435/Lab13/intro.html

[78] H. Kaiser, Guiding concepts relating to trace analysis. InAnalytical Chemistry 4 (1973) 35-61.

[79] http://www.consultrsr.net/resources/eis/diff-o.html

Highlights

SWCNT/SiO_2/Si based highly sensitive electrochemical biosensor is fabricated for Chronic Myeloid Leukemia (CML) detection.

Detection limit of our sensor was found to be 19 cells ml^{-1} which is more superior in comparison to other existing electrochemical sensor.

The fabricated device is cheap and less time consuming in comparison with the available conventional techniques.

The Relative Standard Deviation (RSD) of our immunosensor for two cell concentration i.e $1.5x10^3$ cells ml^{-1} and $1.5x10^5$ cells ml^{-1} range was found to be 3.57% and 2.12% respectively.